198568: Mafic granulite, Jinkas Hill mine

(Youanmi Terrane, Yilgarn Craton)

Blereau, ER, Kelsey, DE and Korhonen, FJ

Location and sampling

DUMBLEYUNG (SI 50-7), KATANNING (2430)

MGA Zone 50, 584193E 6287982N

Warox Site FJKBGD198568

Sampled on 6 June 2010

This sample was collected from Jinkas Hill mine, along Wolyaming road, located about 10.1 km east of Monganining Hill, 9.3 km north of Badgebup, and 0.17 km west of the Jinkas Hill openpit. The sample was collected as part of the Yilgarn Craton Metamorphic Project (2003–14) undertaken by Ben Goscombe for the Geological Survey of Western Australia (GSWA), and referred to in that study as sample BG10-33i. The results from this project have not been released by GSWA, although select data have been published in Goscombe et al. (2019).

Tectonic unit

The unit sampled is a mafic granulite near the western margin of the Youanmi Terrane (Quentin de Gromard et al., 2021). This unit is part of a northwest-trending belt of Archean metasedimentary and gneissic rocks previously assigned to the South West Terrane and referred to informally by Wilde (2001) as the 'Lake Grace domain' (cf. Pidgeon et al., 2010). The boundary between the South West and Youanmi Terranes in this area is a major, northwest-trending shear zone system (Quentin de Gromard et al., 2021). Rock types at the Jinkas Hill Mine and adjacent Dingo prospect (Mukherji, 2012) include intercalated calcalkaline, mafic to felsic volcanic rocks, metamorphosed under upper amphibolite to lower granulite facies conditions. The greenstones have been intruded by post-tectonic granitic rocks (interpreted as similar to adakite or tonalite–trondhjemite–granodiorite (TTG) suite) and by mafic dykes. Gold mineralization is restricted to intermediate to felsic metavolcanic rocks (Mukherji, 2012). A metagranodiorite, sampled from core drilled about 3.9 km to the south-southeast, yielded an igneous crystallization age of 2643 ± 3 Ma, and an age of 2667 ± 2 Ma for the dominant inherited component (GSWA 219901; Lu et al., 2020). A metamonzogranite, sampled about 39 km to the west, yielded an igneous crystallization age of 2669 ± 7 Ma (GSWA 224329, Lu et al., 2019). A metagranodiorite (GSWA 219902; Lu et al., 2020) from drillcore 0.5 km to the northeast records a 2670 ± 5 Ma zircon age interpreted to be magmatic, and a 2635 ± 5 Ma zircon age interpreted to be the age of high-grade metamorphism. Monazite from a felsic gneiss about 32 km to the north-northwest yielded a metamorphic age of 2648 ± 9 Ma (GSWA 198574, preliminary data), and monazite from a pelitic gneiss about 66 km to the northeast yielded a metamorphic age of 2641 ± 6 Ma (GSWA 198585, Fielding et al., 2021b).

Petrographic description

This sample is a medium-grained mafic granulite containing about 46% plagioclase, 35% hornblende, 9% orthopyroxene, 9% clinopyroxene and trace amounts of apatite (Figs 1, 2; Table 1). No Fe–Ti oxides were identified in thin section. Rare orange phlogopite is described for this sample in Goscombe et al. (2019), but was not present in the thin section prepared by GSWA. The sample has an equigranular, polygonal, granoblastic matrix with straight to curvi-planar grain margins and no apparent fabric. Green hornblende, reddish-brown–green orthopyroxene and pale green clinopyroxene are all 1 mm or less in diameter. Plagioclase is of a similar grain size to the mafic minerals and is intergrown with all phases (Figs 1, 2). The sample is homogeneous in hand specimen and shows no evidence for partial melting.

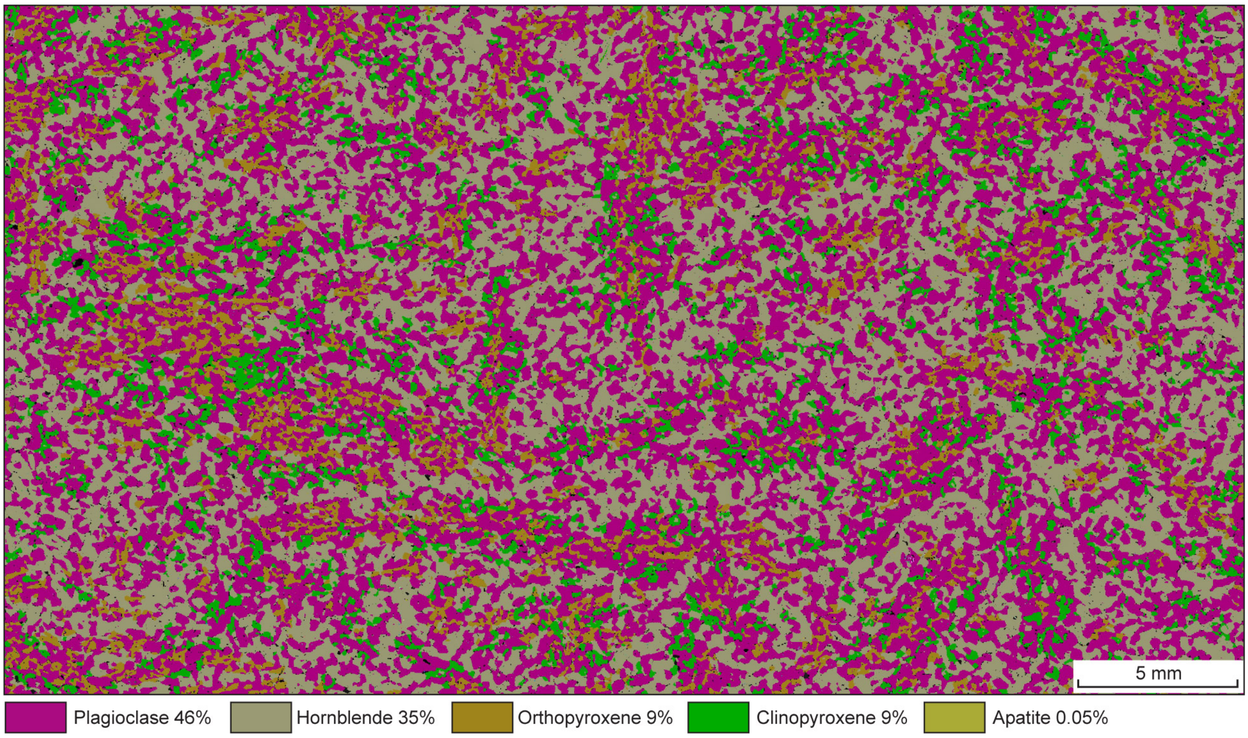

Figure 1. **TESCAN Integrated Mineral Analyser (TIMA) image of an entire thin section from sample 198568: mafic granulite, Jinkas Hill mine. Volume percent proportion of major rock-forming minerals are calculated by the TIMA software**

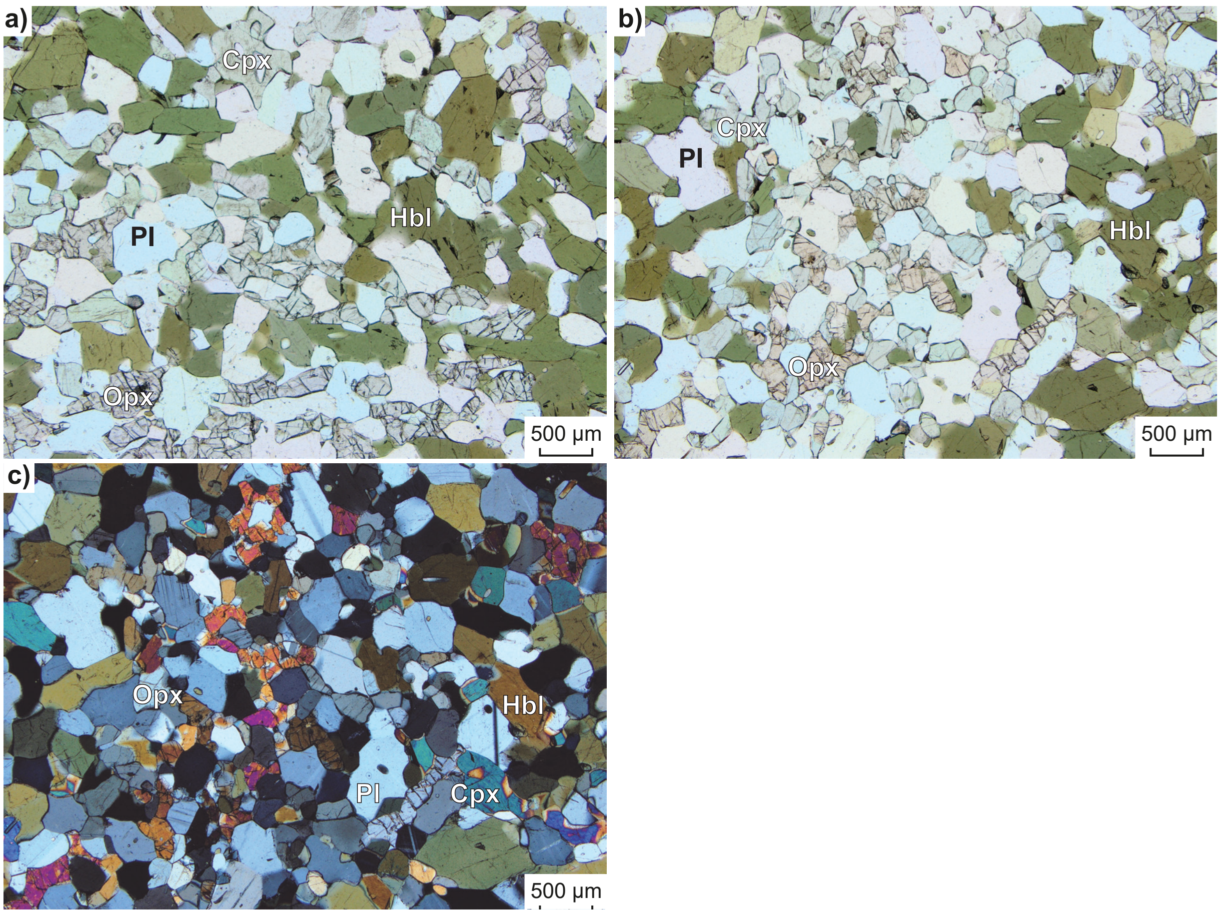

Figure 2. **Photomicrographs, in plane-polarized (a, b) and cross-polarised light (c), of sample 198568: mafic granulite, Jinkas Hill mine. Mineral abbreviations are explained in the caption to Figure 3**

Table 1. Mineral modes for sample 198568: mafic granulite, Jinkas Hill mine

Mineral modes	Pl	Hbl	Opx	Cpx	Ap	Bt	Qz
Observed (vol%)[)]	46	35	9	9	<1	–	–
Predicted (mol%)							
@ 780 °C, 3 kbar	41	33	10	13	–	3	–
@ 820 °C, 5 kbar	40	35	9	14	–	2	–
@ 840 °C, 7.6 kbar	37	37	8	16	–	<1	<1
@ 730 °C, 7 kbar	37	34	10	15	–	2	<1

NOTES: – not present

Methodology and analytical details

Preliminary *P–T* estimates were obtained using multiple-reaction thermobarometry calculated from the mineral compositions (Table 2; Goscombe et al., 2019). These estimates were derived from the 'averagePT' module (avPT) in the program THERMOCALC version tc325 (Powell and Holland, 1988), using the internally consistent Holland and Powell (1998) dataset.

The metamorphic evolution of this sample has been subsequently re-evaluated using phase equilibria modelling, based on the bulk rock composition (Table 3). The bulk rock composition was determined by X-ray fluorescence spectroscopy, together with loss on ignition (LOI). FeO content was analysed by titration, and Fe_2O_3 calculated by difference. The modelled O content (for Fe^{3+}) was derived using these constraints. The modelled H_2O content was based on modal abundance of hornblende in thin section (35.5% containing 2% H_2O, resulting in 0.71 wt%). The bulk composition was corrected for the presence of apatite by applying a correction to calcium (Table 3). Thermodynamic calculations were performed in the NCKFMASHTO (Na_2O–CaO–K_2O–FeO–MgO–Al_2O_3–SiO_2–H_2O–TiO_2–O) system using THERMOCALC version tc340 (Powell and Holland, 1988; updated October 2013) and the internally consistent thermodynamic dataset of Green et al. (2016; version dataset tc-ds63, created January 2015). The activity–composition relations used in the modelling are detailed in Green et al. (2016), with the augite model used for clinopyroxene. Additional information on the workflow with relevant background and methodology are provided in Korhonen et al. (2020).

Table 2. Mineral compositions for sample 198568: mafic granulite, Jinkas Hill mine

Mineral[(a)]	Pl	Pl	Hbl	Hbl	Opx	Opx	Cpx	Cpx	Bt	Bt
Setting	Core	Rim	Core	Rim	Core	Rim	Core	Rim	Core	Rim
wt%										
SiO_2	55.39	53.90	43.23	43.52	52.31	52.92	52.36	52.53	37.25	37.43
TiO_2	0.03	0.01	1.03	1.06	0.00	0.04	0.07	0.11	2.38	2.38
Al_2O_3	27.52	27.69	11.53	11.40	1.41	1.39	2.20	1.97	14.59	14.65
Cr_2O_3	0.01	0.00	0.09	0.07	0.05	0.00	0.03	0.06	0.11	0.08
FeO	0.12	0.16	12.72	12.37	21.70	21.80	8.20	8.28	12.12	12.02
MnO	0.00	0.04	0.18	0.16	0.64	0.58	0.22	0.26	0.05	0.07
MgO	0.00	0.00	13.37	13.61	22.61	23.18	14.20	14.33	17.31	17.63
ZnO	0.02	0.00	0.03	0.03	0.02	0.00	0.00	0.01	0.10	0.06
CaO	10.61	11.38	11.78	11.66	0.56	0.47	22.56	22.48	0.02	0.00
Na_2O	5.56	5.07	1.79	1.62	0.01	0.00	0.46	0.41	0.07	0.04
K_2O	0.34	0.27	1.51	1.45	0.01	0.00	0.01	0.02	9.81	9.95
Total[(b)]	99.59	98.52	97.26	96.95	99.31	100.39	100.29	100.46	93.81	94.31
Oxygen	8	8	23	23	6	6	6	6	11	11
Si	2.51	2.47	6.32	6.36	1.95	1.95	1.93	1.94	2.79	2.79
Ti	0.00	0.00	0.11	0.12	0.00	0.00	0.00	0.00	0.13	0.13
Al	1.47	1.50	1.99	1.96	0.06	0.06	0.10	0.09	1.29	1.29
Cr	0.00	0.00	0.01	0.01	0.00	0.00	0.00	0.00	0.01	0.00
Fe^{3+}[(c)]	0.00	0.00	0.82	0.80	0.03	0.03	0.07	0.06	0.08	0.07
Fe^{2+}	0.00	0.01	0.74	0.71	0.65	0.64	0.19	0.20	0.68	0.67
Mn^{2+}	0.00	0.00	0.02	0.02	0.02	0.02	0.01	0.01	0.00	0.00
Mg	0.00	0.00	2.91	2.97	1.26	1.28	0.78	0.79	1.93	1.96
Zn	0.00	0.00	0.00	0.00	0.00	0.00	0.00	0.00	0.01	0.00
Ca	0.51	0.56	1.84	1.83	0.02	0.02	0.89	0.89	0.00	0.00
Na	0.49	0.45	0.51	0.46	0.00	0.00	0.03	0.03	0.01	0.01
K	0.02	0.02	0.28	0.27	0.00	0.00	0.00	0.00	0.94	0.95
Total	5.00	5.00	15.55	15.50	4.00	4.00	4.00	4.00	7.87	7.87
y(opx)										
Compositional variables										
XFe[(d)]	–	–	0.20	0.19	0.34	0.33	0.19	0.20	0.26	0.26

NOTES: – not applicable
(a) Mineral abbreviations explained in the caption to Figure 2
(b) Totals on anhydrous basis
(c) Hornblende cations calculated following Holland and Blundy (1994); biotite $Fe3^+$ assumed assumed to be 10% of total Fe; Fe^{3+} contents for other minerals based on Droop (1987)
(d) $XFe = Fe^{2+}/(Fe^{2+} + Mg)$

Table 3. Measured whole-rock and modelled compositions for sample 198568: mafic granulite, Jinkas Hill mine

XRF whole-rock composition (wt%)[(a)]												
SiO_2	**TiO_2**	**Al_2O_3**	**Fe_2O_3[(b)]**	**FeO[(c)]**	**MnO**	**MgO**	**CaO**	**Na_2O**	**K_2O**	**P_2O_5**	**LOI**	**Total**
49.46	0.54	16.32	10.09	7.40	0.14	8.86	11.03	2.75	0.49	0.05	0.12	99.85
Normalized composition used for phase equilibria modelling (mol%)												
SiO_2	**TiO_2**	**Al_2O_3**	**O[(d)]**	**FeO^{T}[(e)]**	**MnO**	**MgO**	**CaO[(f)]**	**Na_2O**	**K_2O**	–	**H_2O[(g)]**	**Total**
50.43	0.41	9.80	0.72	7.74	–	13.47	11.98	2.72	0.32		2.41	100

NOTES: (a) Data and analytical details are available from the WACHEM database <http://geochem.dmp.wa.gov.au/geochem/>
(b) Fe_2O_3 content is total Fe
(c) FeO measured by titration
(d) O content (for Fe_2O_3) determined from Fe_2O_3T via the constraint of the FeO titration value
(e) FeO^T = moles FeO + 2 * moles O
(f) CaO modified to remove apatite: CaO(Mod) = CaO(Total) - (moles CaO(in Ap) = 3.33 * moles P_2O_5)
(g) H_2O content is 35.5 vol% hbl * 0.02% H_2O in hbl = 0.071 wt%

Results

Metamorphic *P–T* estimates have been derived based on detailed examination of one thin section and the bulk rock composition; care was taken to ensure that the thin section and the sample volume selected for whole-rock chemistry were similar in terms of featuring the same minerals in approximately the same abundances (Table 1), to minimize any potential compositional differences. The *P–T* pseudosection was calculated over a temperature range of 600–900°C and 2–10 kbar (Fig. 3). The solidus is located between 830–875 °C across the modelled range of pressures. Hornblende, orthopyroxene and clinopyroxene are stable across the modelled pressure and temperature range. Garnet is stable above 6 kbar at 600 °C and 9.7 kbar at 900 °C. Ilmenite is stable below 780 °C at 2 kbar and 700 °C at 7.7 kbar. Rutile is stable above 6.8 kbar at 600 °C and 10 kbar at 735 °C. Quartz is absent at low pressures (below 4.8 kbar at 600 °C) and higher temperatures (above 845 °C at 7.5 kbar). Biotite is stable over much of the *P–T* range, absent only above 845 °C at 7.4 kbar and above 885 °C at 3.3 kbar (Fig. 3).

Metamorphic *P–T* estimates (± 2σ uncertainty) calculated using multiple-reaction thermobarometry are 6.7 ± 2.5 kbar and 672 ± 142 °C (Goscombe et al., 2019). These calculations used the mineral core compositions (Table 2) to estimate peak conditions. Conventional thermobarometry using the hornblende–plagioclase and hornblende–orthopyroxene thermometers reportedly yield similar temperatures, whereas the Al-in-hornblende yields a pressure of 7.6 kbar (Goscombe et al., 2019).

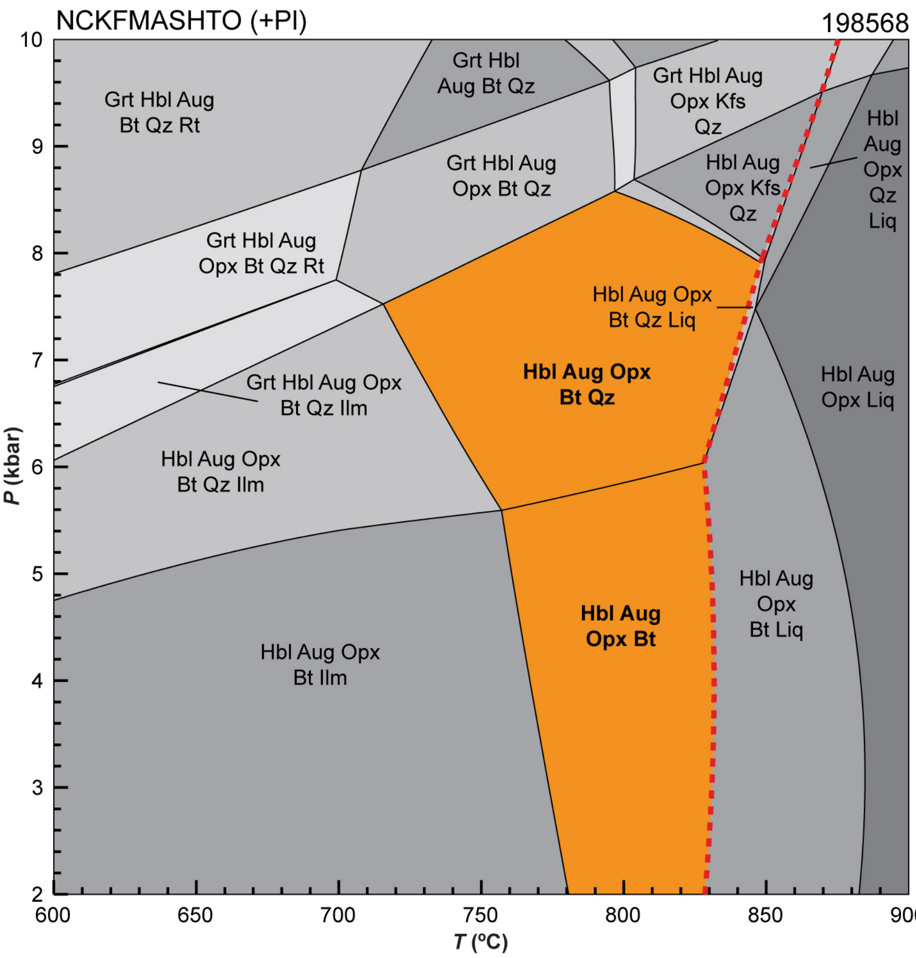

Figure 3. ***P–T*** **pseudosection calculated for sample 198568: mafic granulite, Jinkas Hill mine. Assemblage fields corresponding to peak metamorphic conditions are shown in bold text and orange shading. Red dashed line represents the solidus. Abbreviations: Aug, augite; Bt, biotite; Grt, garnet, Hbl, hornblende; Ilm, ilmenite; Kfs, K-feldspar; Liq, silicate melt; Opx, orthopyroxene; Pl, plagioclase; Qz, quartz; Rt, rutile**

Interpretation

The interpreted peak assemblage of hornblende–clinopyroxene–orthopyroxene–plagioclase implies temperatures were less than those required for partial melting. In the observed thin section there is no biotite, however its predicted stability in the pseudosection is widespread and trace amounts were reported for this sample in Goscombe et al. (2019). The calculated mode of biotite is strongly temperature dependent and decreases from ~3.5% at 650 °C to 0% at its terminal stability at ~850–885 °C. The stability of biotite may be due to the inability of the hornblende activity–composition model to incorporate sufficient K_2O (Forshaw et al., 2019). In addition, the calculated mode of quartz is strongly pressure dependent, and, at 800 °C, increases from 0% at ~5.9 kbar to <1% at ~8.6 kbar where garnet stability commences. Therefore the presence or absence of quartz in the pseudosection does not provide a strong constraint. With these caveats, and the limit of ilmenite stability to lower temperature, melt to higher temperature and garnet to higher pressure, the peak assemblage field is shown as the coloured hornblende–augite–orthopyroxene–plagioclase–biotite(–quartz) fields in Figure 3, which define a *P–T* range of <2.0 – 8.6 kbar and 715−850 °C. There is no petrologic information on the *P–T* path shape and trajectory as the sample records an unretrogressed peak metamorphic mineral assemblage. The results of conventional thermobarometry results occur to lower temperature than these peak fields but overlap within uncertainty.

Peak metamorphic conditions are estimated at 715–850 °C and a maximum pressure of 8.6 kbar, with a minimum apparent thermal gradient of 95 °C/kbar.

References

Droop, GTR 1987, A general equation for estimating Fe^{3+} concentrations in ferromagnesian silicates and oxides from microprobe analyses, using stoichiometric criteria: Mineralogical Magazine, v. 51, no. 361, p. 431–435.

Fielding, IOH, Wingate, MTD, Korhonen, FJ and Rankenburg, K 2021b, 198585: pelitic gneiss, Griffins Find; Geochronology Record 1767: Geological Survey of Western Australia, 5p.

Forshaw, JB, Waters, DJ, Pattison, DRM, Palin, RM and Gopon, P 2019, A comparison of observed and thermodynamically predicted phase equilibria and mineral compositions in mafic granulites: Journal of Metamorphic Geology, v. 37, p. 153–179, DOI: 10.1111/jmg.12454.

Goscombe, B, Foster, DA, Blewett, R, Czarnota, K, Wade, B, Groenewald, B and Gray, D 2019, Neoarchaean metamorphic evolution of the Yilgarn Craton: a record of subduction, accretion, extension and lithospheric delamination: Precambrian Research, article no. 105441, doi:10.1016/j.precamres.2019.105441.

Green, ECR, White, RW, Diener, JFA, Powell, R, Holland, TJB and Palin, RM 2016, Activity-composition relations for the calculation of partial melting equilibria in metabasic rocks: Journal of Metamorphic Geology, v. 34, no. 9, p. 845–869.

Holland, T and Blundy, J 1994, Non-ideal interactions in calcic amphiboles and their bearing on amphibole-plagioclase thermometry: Contributions to Mineralogy and Petrology, v. 116, no. 4, p. 433–447.

Korhonen, FJ, Kelsey, DE, Fielding, IOH and Romano, SS 2020, The utility of the metamorphic rock record: constraining the pressure–temperature–time conditions of metamorphism: Geological Survey of Western Australia, Record 2020/14, 24p.

Lu, Y, Wingate, MTD and Smithies, RH 2019, 224329: metamonzogranite, Trimmer Road; Geochronology Record 1583: Geological Survey of Western Australia, 4p.

Lu, Y, Wingate, MTD and Smithies, RH 2020, 219901: metagranodiorite, Dingo Hill mine; Geochronology Record 1685: Geological Survey of Western Australia, 5p.

Mukherji, A 2012, Katanning South Project: Department of Mines and Petroleum, Mineral Exploration Report A94616, 163p. (unpublished).

Pidgeon, RT, Wingate, MTD, Bodorkos, S and Nelson, DR 2010, The age distribution of detrital zircons in quartzites from the Toodyay– Lake Grace Domain, Western Australia: implications for the early evolution of the Yilgarn Craton: American Journal of Science, v. 310, p. 1115–1135.

Powell, R and Holland, TJB 1988, An internally consistent dataset with uncertainties and correlations: 3. Applications to geobarometry, worked examples and a computer program: Journal of Metamorphic Geology, v. 6, no. 2, p. 173–204.

Quentin de Gromard, R, Ivanic, TJ and Zibra, I 2021, Interpreted bedrock geology of the southwest Yilgarn Craton, Geological Survey of Western Australia, in press.

Wilde, SA 2001, Jimperding and Chittering metamorphic belts, Western Australia - a field guide: Geological Survey of Western Australia, Record 2001/12, 24p.

Links

Metamorphic history introduction document: Intro_2020.pdf

Recommended reference for this publication

Blereau, ER, Kelsey, DE and Korhonen, FJ 2021, 198568: Mafic granulite, Jinkas Hill mine; Metamorphic History Record 9: Geological Survey of Western Australia, 7p.

Data obtained: 21 October 2020

Date released: 25 June 2021

This Metamorphic History Record was last modified on 9 June 2021.

Grid references in this publication refer to the Geocentric Datum of Australia 1994 (GDA94). All locations are quoted to at least the nearest 100 m.

WAROX is GSWA's field observation and sample database. WAROX site IDs have the format 'ABCXXXnnnnnnSS', where ABC = geologist username, XXX = project or map code, nnnnnn = 6 digit site number, and SS = optional alphabetic suffix (maximum 2 characters).

Isotope and element analyses are routinely conducted using the GeoHistory laser ablation ICP-MS and Sensitive High-Resolution Ion Microprobe (SHRIMP) ion microprobe facilities at the John de Laeter Centre (JdLC), Curtin University, with the financial support of the Australian Research Council and AuScope National Collaborative Research Infrastructure Strategy (NCRIS). The TESCAN Integrated Mineral Analyser (TIMA) instrument was funded by a grant from the Australian Research Council (LE140100150) and is operated by the JdLC with the support of the Geological Survey of Western Australia, The University of Western Australia (UWA) and Murdoch University. Mineral analyses are routinely obtained using the electron probe microanalyser (EPMA) facilities at the Centre for Microscopy, Characterisation and Analysis at UWA, and at Adelaide Microscopy, University of Adelaide.

Digital data related to WA Geology Online, including geochronology and digital geology, are available online at the Department's Data and Software Centre and may be viewed in map context at GeoVIEW.WA.

Further details of geoscience products are available from:
Information Centre
Department of Mines, Industry Regulation and Safety
100 Plain Street
EAST PERTH WA 6004
Telephone: +61 8 9222 3459 | Email: publications@dmirs.wa.gov.au
www.dmirs.wa.gov.au/GSWApublications